# Gravitational-Wave Implications for the Parity Symmetry of Gravity at GeV Scale

Yi-Fan Wang[1,2,*], Rui Niu[3,4], Tao Zhu[5,6], Wen Zhao[3,4,†]

[1]Max-Planck-Institut für Gravitationsphysik (Albert-Einstein-Institut), D-30167 Hannover, Germany [2]Leibniz Universität Hannover, D-30167 Hannover, Germany [3]CAS Key Laboratory for Research in Galaxies and Cosmology, Department of Astronomy, University of Science and Technology of China, Hefei 230026, China [4]School of Astronomy and Space Sciences, University of Science and Technology of China, Hefei, 230026, China [5]Institute for theoretical physics and Cosmology, Zhejiang University of Technology, Hangzhou, 310032, China [6]United center for gravitational wave physics (UCGWP), Zhejiang University of Technology, Hangzhou, 310032, China [*]yifan.wang@aei.mpg.de [†]wzhao7@ustc.edu.cn

**Gravitational waves generated by the coalescence of compact binary open a new window to test the fundamental properties of gravity in the strong-field and dynamical regime. In this work, we focus on the parity symmetry of gravity which, if broken, can leave imprints on the waveform of gravitational wave. We construct generalized waveforms with amplitude and velocity birefringence due to parity violation in the effect field theory formalism, then analyze the open data of the ten binary black-hole merger events and the two binary neutron-star merger events detected by LIGO and Virgo collaboration. We do not find any signatures of violation of gravitational parity conservation, thereby setting the lower bound of the parity-violating energy scale to be $0.07$ GeV. This presents the first observational evidence of the parity conservation of gravity at high energy scale, about 17 orders of magnitude tighter than the constraints from the Solar system tests and binary pulsar observation. The third-generation gravitational-wave detector is capable of probing the parity-violating energy scale at $\mathcal{O}(10^2)$ GeV.**

Symmetry is an essential characterization of the fundamental theories of modern physics. Therefore, it is important to test the conservation of these symmetries experimentally. In this work we focus on the parity symmetry which indicates the invariance of physical laws under reversed spatial coordinates. It is well-known that parity is conserved for strong and electromagnetic interactions but is broken in the weak interaction as firstly confirmed by the experiment of beta-decay in cobalt-60 [1]. The gravitational parity is conserved in Einstein's general relativity (GR). Nevertheless, various parity-violating gravity models, including Chern-Simons gravity [2], ghost-free scalar-tensor gravity [3], the symmetric teleparallel equivalence of GR theory [4] and Hořava-Lifshitz gravity [5,6] have been proposed for different motivations. In particular, in some fundamental theories of gravity, such as string theory and loop quantum gravity, the parity violation in the high energy regime is inevitable [2]. However, the observational evidence for gravity at high energy scale is limited. In this work we report the first evidence for gravitational parity conservation at GeV scale from the gravitational wave (GW) observation.

We first construct the generalized GW waveform generated by compact binary coalescence (CBC) with parity violation using the effective field theory (EFT) formalism. In particular, we assume all modifications to GR-based GW waveform only arise from the propagation effect, and ignore the parity-violating generation effect caused by a modified energy loss, inspiral rate, and chirping rate of the binaries. This assumption is justified since the generation effect occurs on a radiation-reaction timescale, which is much smaller than the GW time of flight, thus its impact on the evolution of the GW waveform is negligible [7].

EFT provides a systematic framework to encode all kinds of modifications to an existing theory that could arise given certain new physics, thus simultaneously testing a range of modified gravity theories at once. To investigate the possible propagation effect due to parity violation, we consider the perturbation theory of gravitational field. Compared with GR, EFT suggests that the leading-order modification comes from two terms with three derivatives, i.e., $\epsilon^{ijk}\dot{h}_{il}\partial_j\dot{h}_{kl}$ and $\epsilon^{ijk}\partial^2 h_{il}\partial_j h_{kl}$ with $\epsilon^{ijk}$ the antisymmetric symbol and $h_{ij}$ the tensor perturbation of metric, $\partial_j$ and a *dot* denote the derivatives with respect to spatial coordinates and time, respectively [8]. Both terms are parity-violating. Dimensional analysis dictates that these new terms are each suppressed by an energy scale $M_{\rm PV}$. This EFT with leading-order extensions to GR can describe the GW propagation effect with parity violation from all the existing modified gravity models in the market [9].

Given the parity-violating terms, the equation of motion for the GW circular polarization mode $h_A$ in a Friedmann-Robertson-Walker (FRW) Universe is

$$h''_A + (2+\nu_A)\mathcal{H}h'_A + (1+\mu_A)k^2 h_A = 0\,, \tag{1}$$

where $A = L$ or $R$ stands for the left- and right-hand modes, $\mathcal{H}$ is the Hubble parameter, $k$ is the wave-number, a prime denotes the derivative with respect to the conformal cosmic time. Note that $\mu_A = \nu_A = 0$ would reduce Eq. (1) to GR. The emergence of the term $\mu_A$ and $\nu_A$ is due to the parity violation effect. Dimensional analysis induces that both terms relate to the energy scale by $\mu_A \propto \rho_A k/M_{\rm PV}$ and $\nu_A \propto \rho_A k/M_{\rm PV}$ with $\rho_R = 1$ and $\rho_L = -1$, the broken parity leads to asymmetry between the left- and right-hand circular polarization modes of GW during propagation. In particular, the opposite sign of $\mu_A$ (as well as $\nu_A$) for different modes leads to the birefringence effect of GWs, which is a characterized phenomenon for GW propagation in the parity-violating gravity. We find that the parity violation can affect the propagation of the GWs in two ways. The term $\mu_A$ modifies the conventional dispersion relation of the GWs. As a result, the velocities of left- and right-hand circular polarization of GWs are different. This phenomenon is always called the *velocity birefringence* of GWs. On the other hand, the term $\nu_A$ induces the different damping rates for two polarization modes when they propagate in the expanding universe, which is called the *amplitude birefringence* of GWs. In the general parity-violating gravities, both effects exist during the propagation of GWs in the universe. For each circular polarization mode, the former effect exactly induces the phase modifications of the GW waveform, and the latter one induces the amplitude modifications.

The parity-violating GW waveform in the frequency domain can be expressed by

$$h_A^{\rm PV}(f) = h_A^{\rm GR}(f)\,(1+\rho_A\delta h)\,e^{i\rho_A\delta\Psi}\,, \tag{2}$$

where $f$ is the frequency, and $\delta h$ and $\delta\Psi$ are induced by $\nu_A$ and $\mu_A$, respectively. It should also be noted that since $\delta\Psi$ is larger than $\delta h$ by about 20 order of magnitude [9], it is safe to only take into account the contribution of $\delta\Psi$. But we also consider the special scenario where the amplitude birefringence is the only modification to the GR waveform, i.e., $\delta\Psi = 0$ as is the case for, e.g., Chern-Simons gravity.

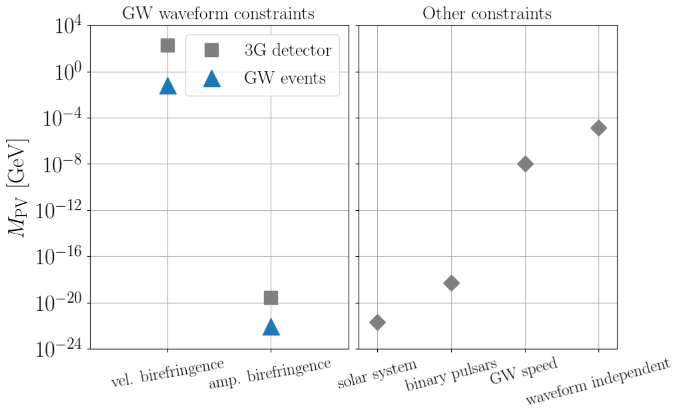


**Figure 1 | Current and potential lower limits of the parity-violating energy scales in gravity from various observations.** The left panel includes the results from twelve CBC events and the projected results of third-generation detector network. The right panel includes the results from the LAGEOS satellite in Solar system [10], that from the double pulsar system PSR J0737-3039 A/B [12], that from the arrival time difference between GW170817 and GRB170817A, and the potential result by considering the waveform-independent method developed in [29].

With the waveform Eq. (2), we can perform a direct comparison with the GW data using Bayesian inference to investigate the parity violation effect. Up to date, LIGO and Virgo collaboration has detected and released twelve confident CBC events. The catalog GWTC-1 from the first and second observation runs include ten binary black hole (BBH) events and a binary neutron star (BNS) event GW170817 [14]. Recently, a second BNS event, GW190425, has been released [15]. We analyze the open data [16] of the twelve confident events with the inference module of the open-source software `PyCBC` [17]developed for GW astronomy, which in turn has dependency on `LALSuite` [18].

For all the GW events, we do not find any signatures of parity violation by comparing the Bayes evidence of the parity-violating gravity with that of GR. Our inference results of the constraint on $M_{\rm PV}$ with GW events are shown in Fig. 1, where we have combined the constraints from the twelve CBC events. It can be seen that the lower limit of $M_{\rm PV}$ is 0.07 GeV in the general parity-violating models with velocity birefringence effect. This is tighter than the constraint from the Solar system and binary pulsar observation by 17 order of magnitude. The reason of this dramatic improvement is that, the velocity birefringence effect in the modification of GW waveforms is accumulated during the propagation of GW signals, and can be greatly amplified for the distant GW events. We note that this result has direct application on constraining a range of specific parity-violating gravity models with velocity birefringence, including the ghost-free scalar-tensor gravity [3], the symmetric teleparallel equivalence of GR theory [4] and Hořava-Lifshitz gravity [5,6]. The detailed correspondence between the above modified gravity models and the EFT formalism can be found in Ref. [9]. By similar analysis, the constraint by only considering the amplitude birefringence modification is $M_{\rm PV} > 1 \times 10^{-22}$ GeV. This result is consistent with Ref. [31] which focuses on testing Chern-Simons gravity with GW. Compared to the constraint from velocity birefringence, the loose result for amplitude birefringence is because $\delta h$ is negligibly small compared with $\delta\Psi$ and the GW detection is less sensitive to amplitude modification.

With the continuing sensitivity upgrade during the advanced LIGO and Virgo runs, we expect the future more detections from CBC events will further improve the constraints on $M_{\rm PV}$. We also forecast the projected constraints on $M_{\rm PV}$ from GW measurements in the third-generation detector era if there is no parity-violation detections. We consider a detector network consisting of one Einstein Telescope (ET) in Europe [26] and one Cosmic Explorer (CE) in the U.S. [27]. Using Fisher information matrix approach [28], we consider a GW170817-like source with equal component mass $1.4M_\odot$, distance 40 Mpc and the optimal spatial direction. As shown in Fig. 1, the third generation detectors can put the lower limit of $M_{\rm PV}$ with velocity birefringence to be $\mathcal{O}(10^2)$ GeV. In comparison with the current constraints, the bound of $M_{\rm PV}$ is improved by three orders of magnitude. For the parity-violating gravity with only amplitude birefringence, the constraints on $M_{\rm PV}$ by the third-generation detector is improved to $\mathcal{O}(10^{-20})$ GeV.

We note that other constraints on the violation of parity symmetry of gravity have also been derived in various analysis using GW or non-GW observations. In the following, we briefly summarize these results to describe the status-of-the-art of the constraint on $M_{\rm PV}$. The results are also presented in the Fig. 1 as a comparison of our work.

*Waveform-independent constraint from GWs*: Our previous work Ref. [29] develops a waveform-independent way to decompose the left- and right-hand polarization modes from the observed GW data if the sky position of the event can be fixed by the observation of its electromagnetic counterparts. From the frequency-time representations we can readout the arrival times of GW in each frequency band. According to the velocity birefringence effect, for a specific frequency $f$, the arrival time difference between the two modes is $|t_{\rm R-L}| = (2\pi f/M_{\rm PV})^2 \int_{t_e}^{t_0} a^{-2} dt$, where $a$ is the scale factor of the universe, $t_0$ and $t_e$ are the cosmic time of the arrival and the emission of the GW event respectively. This formula gives a direct relation between the arrival time difference and the energy scale of parity violation $M_{\rm PV}$. Applying to the mock data, we find that if a nearly edge-on BNS at 40 Mpc is detected by the second-generation detector network consisting of advanced LIGO, advanced Virgo, KAGRA, and LIGO-India, one could derive the waveform-independent bound $M_{\rm PV} > 1.4 \times 10^4$ eV. At this writing, the BNS signal GW170817 is the unique GW event with observed electromagnetic counterparts. However, this event is nearly face-on with the inclination angle $\iota \geq 152^\circ$ [23], thus the right-hand mode of this event is completely dominant. Therefore, the difference of the arrival time between the two modes can not be determined from GW170817.

*Constraint from GW speed*: The velocity birefringence effect of GW can be constrained from the speed of GW, which in turn can be obtained by comparing the arrival time of GW signal and that of the electromagnetic signal. For the event GW170817/GRB170817A, the arrival time difference between GW and gamma-ray burst is 1.7 seconds. Assuming the difference of their emission time is less than 10 seconds, the speed of the right-hand circular mode of GW is in the range $-7 \times 10^{-16} < 1 - v_R < 3 \times 10^{-15}$ [30]. According to the relation $|v_R - 1| = \pi f/M_{\rm PV}$, one can obtain the constraint $M_{\rm PV} \gtrsim 10$ eV, which is consistent with the result in Ref.[24].

*Constraint from Solar system tests*: In the parity-violating gravity, an important feature is that it leads to a change of frame-dragging effects around rotating objects, which can be used to test the theory. Focusing on the Chern-Simons gravity, Ref. [10] calculates the linearized metric of the spacetime around a non-relativistic, constant-density spinning body. It is found that the gravitomagnetic field in the parity-violating gravity differs from that in GR, which induces the modifications in the precession of orbits of gyroscopes moving in this spacetime. Using the measurement of Lense-Thirring drag around the Earth by the LAGEOS satellites, Ref. [10] sets the constraint on the characteristic Chern-Simons length scale, $k_{\rm CS}^{-1} \lesssim 1000$ km, which corresponds to $M_{\rm PV} \gtrsim 2 \times 10^{-13}$ eV.

*Constraint from binary pulsar*: In the parity-violating gravity, the theory selects a preferred direction in spacetime that corrects the precession of the orbital plane. Thus, observations of gravitomagnetic precession can be used to test the validity of the theory. In Refs.[11,12], the authors focus on the Chern-Simons modified gravity with a timelike Chern-Simons coupling scalar field, and calculate the leading-order correction to the post-Keplerian parameters of binary systems. They find that the precession of the periastron is corrected by the parity-violating term. Using the measurements of the rate of periastron precession in the double pulsar system PSR J0737-3039 A/B, they obtain a constraint of $k_{\rm CS}^{-1} \lesssim 0.4$ km, which corresponds to $M_{\rm PV} \gtrsim 5\times10^{-10}$ eV. Note that the constraints of $M_{\rm PV}$ from the measurements of Solar system and binary pulsar are based on the effect of frame-dragging modifications in the theory, which is the local effect rather than the propagation effect. Since the frame-dragging modification around rotating objects is a common feature for all the parity-violating gravities, although these constraints are derived for a specific parity-violating theory, i.e. Chern-Simons gravity, we expect that the conclusions are applicable for other theories of parity-violating gravity.

Y.-F.W thanks Badri Krishnan and Collin Capano for the fruitful discussion and acknowledges the Max Planck Gesellschaft for support and the Atlas cluster computing team at AEI Hannover. W.Z and R.N. appreciate the helpful discussion with Linqing Wen, Xing Zhang, Qian Hu, Mingzheng Li and Anzhong Wang. W.Z. is supported by NSFC Grants No. 11773028, No. 11633001, No. 11653002, No. 11421303, No. 11903030, and the Strategic Priority Research Program of the Chinese Academy of Sciences Grant No. XDB23010200. T.Z. is supported in part by NSFC Grants No. 11675143, the Zhejiang Provincial NSFC Grant No. LY20A050002, and the Fundamental Research Funds for the Provincial Universities of Zhejiang in China Grants No. rf-a2019015. This research has made use of data, software and/or web tools obtained from the Gravitational Wave Open Science Center (https://www.gw-openscience.org), a service of LIGO Laboratory, the LIGO Scientific Collaboration and the Virgo Collaboration. LIGO is funded by the U.S. National Science Foundation. Virgo is funded by the French Centre National de Recherche Scientifique (CNRS), the Italian Istituto Nazionale della Fisica Nucleare (INFN) and the Dutch Nikhef, with contributions by Polish and Hungarian institutes.

**Methods**

In what follows we present our method for inferring the constraint on parity violation in gravity from GW measurements. We first introduce the explicit GW waveforms from CBC with parity violation in the EFT framework, then discuss the Bayesian inference to obtain the constraint with the twelve CBC events. Last we use Fisher information matrix to forecast the projected constraint in the third-generation detector era.

**GW waveform** In this part we follow Refs. [8,9,29] to briefly review the explicit GW waveform with parity-violation in the EFT framework. In the FRW universe, the equation of motion of GW is determined by the following quadratic action [8]

$$S=\frac{1}{16\pi G}\int dt d^3x a^3\left[\frac{1}{4}\dot{h}_{ij}^2-\frac{1}{4a^2}(\partial_k h_{ij})^2+\frac{1}{4}\left(\frac{c_1}{aM_{\rm PV}}\epsilon^{ijk}\dot{h}_{il}\partial_j\dot{h}_{kl}+\frac{c_2}{a^3M_{\rm PV}}\epsilon^{ijk}\partial^2 h_{il}\partial_j h_{kl}\right)\right], \tag{3}$$

where the last two terms with three derivatives correspond to the contribution from parity violation. $c_1$ and $c_2$ are dimensionless coefficients, which are functions respective to cosmic time in general. From the action we can derive the equation of motion of GWs in the vacuum as shown in Eq. (1). The exact forms for $\mu_A$ and $\nu_A$ are [9]

$$\begin{aligned}\nu_A &= [\rho_A\alpha_\nu(\tau)(k/aM_{\rm PV})]'/\mathcal{H},\\ \mu_A &= \rho_A\alpha_\mu(\tau)(k/a\,M_{\rm PV}),\end{aligned} \tag{4}$$

where $\tau$ is the cosmic conformal time. The functions $\alpha_\nu\equiv -c_1$ and $\alpha_\mu\equiv c_1-c_2$ are two arbitrary functions of time which can only be determined given a specific model of modified gravity. For the GW events at local Universe, these two functions can be approximately treated as constant, i.e. ignoring their time-dependence. Note that we consider $\alpha_\mu$ and $\alpha_\nu$ are $\sim\mathcal{O}(1)$ by absorbing the order of magnitude into $M_{\rm PV}$.

The explicit parity-violating GW waveform can be derived from solving the equation of motion, as schematically shown by Eq. (2). The amplitude and phase modifications to the GR-based waveform due to birefringence take the following parametrized form

$$\delta h(f)=-A_\nu\pi f,\;\; \delta\Psi(f)=A_\mu(\pi f)^2/H_0, \tag{5}$$

where $H_0$ is the Hubble constant. The coefficients $A_\nu$ and $A_\mu$ are given by

$$\begin{aligned}A_\nu &= M_{\rm PV}^{-1}\left[\alpha_\nu(z=0)-\alpha_\nu(z)(1+z)\right],\\ A_\mu &= M_{\rm PV}^{-1}\int_0^z\frac{\alpha_\mu(z')(1+z')dz'}{\sqrt{\Omega_M(1+z')^3+\Omega_\Lambda}},\end{aligned} \tag{6}$$

where $z$ is the redshift of GW event. In analysis we adopt a Planck cosmology ($\Omega_M=0.308,\Omega_\Lambda=0.692,H_0=67.8$ km/s/Mpc) .

We also convert the left- and right-hand GW polarization modes into the *plus* and *cross* modes which are used more often in the context of GW data analysis. The relation between the parity-violating modes and the GR modes is

$$\begin{aligned}h_+^{\rm PV}(f) &= h_+^{\rm GR}(f)-h_\times^{\rm GR}(f)(i\delta h-\delta\Psi),\\ h_\times^{\rm PV}(f) &= h_\times^{\rm GR}(f)+h_+^{\rm GR}(f)(i\delta h-\delta\Psi).\end{aligned} \tag{7}$$

The above expression represents the waveform we use to compare with the GW data.

**Bayesian inference with GW observation** Bayesian inference is broadly used in the field of GW astronomy for parameter estimation and model selection. Given the data $d$ of the GW strain from detectors, Bayes theorem claims

$$P(\vec{\theta}|d,H,I)=\frac{P(d|\vec{\theta},H,I)P(\vec{\theta}|H,I)}{P(d|H,I)}, \tag{8}$$

where $H$ is the assumed theoretical model which is GR or parity-violating gravity models in this work. $\vec{\theta}$ are the parameters characterizing $H$, $I$ is any other background information. $P(\vec{\theta}|H,I)$ is the prior distribution for $\vec{\theta}$ and $P(d|\vec{\theta},H,I)$ is the likelihood for obtaining the data from a specific set of model parameters. The posterior $P(\vec{\theta}|d,H,I)$ contained all the information about the results of parameter estimation.

The GW detector noise is assumed to be Gaussian and stationary, therefore the likelihood function is

$$P(d|\vec{\theta},H,I)=\exp\left[-\frac{1}{2}\sum_{i=1}^{N}\langle d-h(\vec{\theta})|d-h(\vec{\theta})\rangle\right], \tag{9}$$

where $h(\vec{\theta})$ is the GW waveform template for parity-violating gravity. The inner product $\langle a|b\rangle$ is

$$\langle a|b\rangle=4\Re\int\frac{a(f)b^*(f)}{S_h(f)}df, \tag{10}$$

where $S_h(f)$ is the one-side noise power spectral density (PSD) of the GW detectors.

To select the model favored by observation $d$, normalizing both sides of Eq. (8), the Bayes evidence can be obtained

$$P(d|H,I) = \int d\vec{\theta} P(d|\vec{\theta},H,I) P(\vec{\theta}|H,I). \tag{11}$$

Bayesian ratio is defined as the ratio of evidence of two competitive models $H_1$ and $H_2$

$$\mathcal{B}_2^1 = \frac{P(d|H_1,I)}{P(d|H_2,I)}. \tag{12}$$

The odds ratio between model $H_1$ and model $H_2$ can be expressed by

$$\mathcal{O}_2^1 = \frac{P(H_1|d,I)}{P(H_2|d,I} = \frac{P(d|H_1,I)}{P(d|H_2,I)} \frac{P(H_1|I)}{P(H_2|I)} = \mathcal{B}_2^1 \frac{P(H_1|I)}{P(H_2|I)}. \tag{13}$$

If the competitive models are assumed to be equally likely before any measurement, then odds ratio is equal to Bayesian ratio.

In this work, we use the inference module of the open-source software `PyCBC` with the open data from [16]. For the GR waveform $h^{\rm GR}(f)$, we use the `IMRPhenomPv2` [19,20] waveform for analyzing BBH events and `IMRPhenomD_NRTidal` [21] for BNS events. The parity-violating waveform is constructed based on the above template through Eq.(7). We perform parameter estimation by selecting 16s data for BBH and 200s data for the two BNS events to account for the long waveform. The data is sampled at 2048 Hz and the likelihood is evaluated between 20 Hz and 1024 Hz. The PSD is generated from 1000s data using the median estimation with 8s Hann-windowed segments and overlapped by 4s [17]. The posterior distribution are sampled by the nest sampling software `dynesty` [22] over the fiducial BBH and BNS source parameters plus the parity-violating parameters $A_\mu$ for velocity birefringence or $A_\nu$ for amplitude birefringence. Since we do not find violation of GR and aim for putting a lower limit to $M_{\rm PV}$, we ignore the calibration error from GW detectors, thus our lower limit should be interpreted as a conservative result for constraining $M_{\rm PV}$. Other settings can be found in our released data.

Fig. 2 shows the marginalized posterior distribution for $A_\mu$ for velocity birefringence. From the figure we can see that the GR value $A_\mu = 0$ is within the 90% confidence level for every event. We also numerically verified that the Bayes ratio between the parity-violating gravity and GR is larger than $\exp(5)$ for every event, which provides the evidence for gravity parity conservation from GW observation.

The relatively low-mass BBH events, such as GW151226, GW170608, GW170814 and the two BNS events give tighter constraint on $A_\mu$. This is because the velocity birefringence contribution corresponds to a 5.5 post-Newtonian (PN) order modification to the GR waveform. Therefore, the low-mass events with higher cut-off frequency and longer waveform have better constraints on such a high PN order contribution.

For converting $A_\mu$ into $M_{\rm PV}$, we absorb the absolute value of $\alpha_\mu$ into the definition of $M_{\rm PV}$, which is equivalent to set $|\alpha_\mu| = 1$ in the calculation. Afterwards, the parameter $M_{\rm PV}$ can be converted from $A_\mu$ and redshift $z$ by Eq. (6). The cumulative posterior distribution of $M_{\rm PV}$ for each event is shown in Fig. 3. It is straightforward to combine the posterior on $M_{\rm PV}$ from each event to give an overall constraint with all GW events by

$$p(M_{\rm PV}|\{d_i\},H,I) \propto \prod_{i=1}^{N} p(M_{\rm PV}|d_i,H,I) \tag{14}$$

where $d_i$ denote the i-th GW event. We can observe that the 90% lower limit for $M_{\rm PV}$ is 0.07 GeV. This represents the first observational confirmation of gravitational parity conservation in GeV scale.

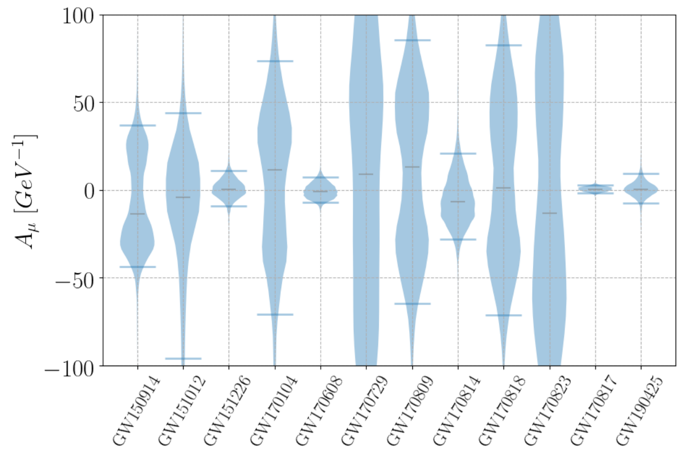


**Figure 2 | Violin plots of the full posteriors on the parameter $A_\mu$** The results are obtained from the twelve GW events, the region between the upper and lower bar denote the 90% credible interval, the bar at the middle of each posterior denotes the median value. The GR value $A_\mu = 0$ is within the 90% confidence interval for each event.

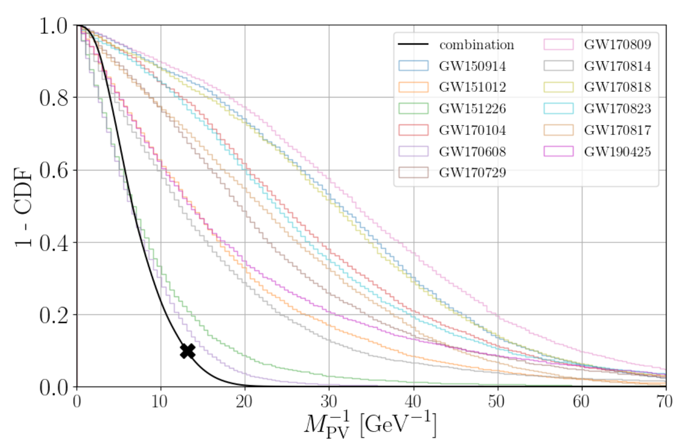


**Figure 3 | The reversed cumulative density distribution (CDF) for $M_{\rm PV}^{-1}$.** The inference results for the parity-violating energy scale for velocity birefringence are plotted. Both the results from individual GW event and the combination of all the events are considered. The abscissa value of the “x” marker represents the 90% lower limit for $M_{\rm PV}$, which is 0.07 GeV.

**Forecasts for third-generation detectors** In order to estimate the potential constraint by the future GW observation in the third-generation detector era, we employ the Fisher matrix approach [28]. It has been shown that Fisher matrix is accurate enough to estimate the parameter in high signal-to-noise ratio regime, which is the case for the third generation GW detectors. In the case of a single interferometer $a$ ($a = 1, 2, 3, \cdots$), the Fisher matrix is given by

$$\Lambda^a_{ij} = \langle h^a_i(f)|h^a_j(f)\rangle, \;\; h^a_i \equiv \partial h^a(f)/\partial\theta_i, \tag{15}$$

where $\theta_i$ denote the free parameters to be estimated. We consider an assumed third-generation detector network consisting of one ET (including three interferometers) in Europe and one CE in the U.S.. The Fisher matrix for the combination of the individual interferometers is the sum of the individual ones. Once the total Fisher matrix $\Lambda_{ij}$ is derived, an estimate of root-mean-square error, $\Delta\theta_i$, in measuring the parameter $\theta_i$ can then be calculated in the limit of large signal-to-noise ratio, by taking the square root of the diagonal elements of the inverse of the Fisher matrix, i.e. $\Delta\theta_i = (\Lambda^{-1})^{1/2}_{ii}$.

In this work, we investigate how the constraint on $M_{\rm PV}$ depends on total mass and luminosity distance of GW sources. Since the effects of velocity birefringence are much more significant than amplitude birefringence as discussed, we consider the case in which only the phase birefringence is included. The masses of two components are assumed to be equal and the sky position is chosen to be the optimal direction for the detection.

The result is shown in the Fig. 4. We consider a mass range of $[5, 50]M_\odot$ and a redshift range of $[0.01, 1]$. For the nearest and lightest sources, the constraints can reach to $\mathcal{O}(10^2)$ GeV. A noticeable feature is that for the sources at a fixed redshift $z$, as the mass increasing, the constraints become worse first but turn better for heavy sources. For lighter binaries, the longer waveform is beneficial to constrain $M_{\rm PV}$, while the heavier binaries have larger signal-to-noise ratio. We also plot the signal-to-noise ratio in Fig. 4 to show this trend.

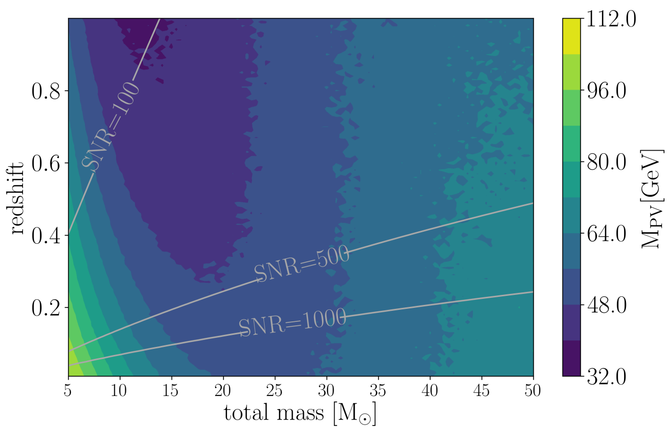


**Figure 4 | The projected constraints for $M_{\rm PV}$ from the third-generation GW detectors.** Assuming there is no parity-violation, the constraint for the lower limit of the parity-violating energy scale for velocity birefringence is plotted. The best constraint come from the nearest and the lightest source, which gives $M_{\rm PV} > \mathcal{O}(10^2)$ GeV.


1. T. D. Lee and C. N. Yang, Phys. Rev. **104**, 254 (1956).
2. S. Alexander and and N. Yunes, Phys. Rep. **07**, 002 (2009).
3. M. Crisostomi, K. Noui, C. Charmousis and D. Langlois, Phys. Rev. D **97**, 044034 (2018).
4. A. Conroy and T. Koivisto, JCAP **12**, 016 (2019).
5. P. Horava, Phys. Rev. D **79**, 084008 (2009).
6. A. Wang, Q. Wu, W. Zhao and T. Zhu, Phys. Rev. D **87**, 103512 (2013).
7. S. H. Alexander and N. Yunes, Phys. Rev. D **97**, 064033 (2018).
8. P. Creminelli, J. Gleyzes, J. Norena and F. Vernizzi, Phys. Rev. Lett. **113**, 231301 (2014).
9. W. Zhao, T. Zhu, J. Qiao and A. Wang, Phys. Rev. D **101**, 024002 (2020).
10. T. L. Smith, A. L. Erickcek, R. R. Caldwell and M. Kamionkowski, Phys. Rev. D **77**, 024015 (2008).
11. N. Yunes and D. N. Spergel, Phys. Rev. D **80**, 042004 (2009).
12. Y. Ali-Haimoud, Phys. Rev. D **83**, 124050 (2011).
13. A. Kostelecky and M. Mewes, Phys. Lett. B **757**, 510 (2016).
14. B. P. Abbott et al. (LIGO Scientific and Virgo Collaborations), Phys. Rev. Lett. **119**, 141101 (2017).
15. B. P. Abbott *et al.* [LIGO Scientific and Virgo Collaborations], arXiv:2001.01761 [astro-ph.HE].
16. M Vallisneri et al. "The LIGO Open Science Center", proceedings of the 10th LISA Symposium, University of Florida, Gainesville, May 18-23, 2014; also arXiv:1410.4839
17. C. M. Biwer, C. D. Capano, S. De, M. Cabero, D. A. Brown, A. H. Nitz and V. Raymond, Publ. Astron. Soc. Pac. **131**, no. 996, 024503 (2019)
18. LIGO Scientific Collaboration, "LIGO Algorithm Library - LALSuite", free software (GPL), doi= "10.7935/GT1W-FZ16", (2018)
19. P. Schmidt, F. Ohme and M. Hannam, Phys. Rev. D **91**, no. 2, 024043 (2015)
20. M. Hannam, P. Schmidt, A. Bohé, L. Haegel, S. Husa, F. Ohme, G. Pratten and M. Pürrer, Phys. Rev. Lett. **113**, no. 15, 151101 (2014)
21. T. Dietrich, S. Bernuzzi and W. Tichy, Phys. Rev. D **96**, no. 12, 121501 (2017)
22. Joshua S Speagle, Monthly Notices of the Royal Astronomical Society, staa278,
23. B. P. Abbott et al. (LIGO Scientific and Virgo Collaborations), Phys. Rev. Lett. **119**, 161101 (2017).
24. A. Nishizawa and T. Kobayashi, Phys. Rev. D **98**, 124018 (2018).
25. J. Qiao, T. Zhu, W. Zhao and A. Wang, Phys. Rev. D **100**, 124058 (2019).
26. M. Punturo et al., Classical Quantum Gravity **27**, 194002 (2010).
27. B. P. Abbott et al., Classical Quantum Gravity **34**, 044001 (2017).
28. L. Wen and Y. Chen, Phys. Rev. D **81**, 082001 (2010).
29. W. Zhao, T. Liu, L. Q. Wen, T. Zhu, A. Wang, Q. Hu and C. Zhou, arXiv:1909.13007.
30. LIGO Scientific Collaboration, Virgo Collaboration, Fermi Gamma-Ray Burst Monitor, INTEGRAL, Astrophys. J. Lett., **848**, L13 (2017).
31. K. Yagi and H. Yang, Phys. Rev. D **97**, 104018 (2018).
32. J. Qiao, T. Zhu, W. Zhao and A. Wang, Phys. Rev. D **100**, 124058 (2019).
33. S. H. Alexander and N. Yunes, Phys. Rev. D **97**, 064033 (2018).
34. K. Throne, in *300 Years of Gravitation*, Edited by S. Hawking and W. Isreal, Cambridge University Press, (1987).
35. B. P. Abbott et al. (LIGO Scientific and Virgo Collaborations), Phys. Rev. D **100**, 104036 (2019).
36. W. Zhao and L. Wen, Phys. Rev. D **97**, 064031 (2018).


**Data release** The posterior files for velocity and amplitude birefringence of the twelve GW events are released in https://github.com/yi-fan-wang/ParitywithGW